

Structure–Function Relationships in Unsymmetrical Zinc Phthalocyanines for Dye-Sensitized Solar Cells

Juan-José Cid,^[a] Miguel García-Iglesias,^[a] Jun-Ho Yum,^[b] Amparo Forneli,^[c] Josep Albero,^[c] Eugenia Martínez-Ferrero,^[c] Purificación Vázquez,^[a] Michael Grätzel,^[b] Mohammad K. Nazeeruddin,^{*[b]} Emilio Palomares,^{*[c]} and Tomás Torres^{*[a]}

Abstract: A series of unsymmetrical zinc phthalocyanines bearing an anchoring carboxylic function linked to the phthalocyanine ring through different spacers were designed for dye-sensitized solar cells (DSSC). The modification of the spacer group allows not only a variable distance between the dye and the nanocrystalline TiO₂, but also a distinct orientation of the phtha-

locyanine on the semiconductor surface. The photovoltaic data show that the nature of the spacer group plays a significant role in the electron injection from the photo-excited dye into the

nanocrystalline TiO₂ semiconductor, the recombination rates and the efficiency of the cells. The incident monochromatic photon-to-current conversion efficiency (IPCE) for phthalocyanines bearing an insulating spacer is as low as 9%, whereas for those with a conducting spacer an outstanding IPCE 80% was obtained.

Keywords: electron transfer • mesoporous materials • photochemistry • phthalocyanines • sensitizers • zinc

Introduction

Phthalocyanines^[1] are an active focus of intense research for the development of efficient light-to-energy conversion devices.^[2–13] Such molecules have unique properties in terms of light absorption in the far visible region of the solar spectrum ($\lambda = 690$ nm) with molecular extinction coefficients (ϵ) higher than $100\,000\text{ dm}^3\text{ M}^{-1}\text{ cm}^{-1}$ and good chemical stability.

Moreover, through the rational design of their structure, we have previously shown the possibility of controlling their electrochemical and photophysical properties.^[14,15] Also, we have demonstrated the possibility of controlling the electron recombination dynamics between nanocrystalline TiO₂ particles and axially anchored titanium phthalocyanines.^[15] However, despite the number of groups working on the development of phthalocyanines for molecular photovoltaic devices, only recently have there been reports of efficiencies higher than 3% under standard conditions (100 mW cm^{-2} , air mass (AM) 1.5).^[9,10] Previously, Hagfeldt et al. showed that the formation of molecular aggregates of zinc phthalocyanines was a major issue for the achievement of reasonable efficiencies.^[7] Such aggregates are formed on the surface of the nanoparticles, avoiding efficient electron injection into the semiconducting band when the sensitised film is irradiated. In fact, the use of co-adsorbents, such as chenodeoxycholic acid, reduces the formation of such aggregates, but does not drastically increase the device efficiency. Hence, other key factors might also have an important influence over the charge-transfer reaction that takes place at the different interfaces of the dye-sensitized solar cells. We recently showed that the design of the peripheral substituents such as *tert*-butyl groups on the phthalocyanine ring was paramount to reducing the formation of aggregates onto the TiO₂ surface and thereby achieving incident photon-to-current efficiencies (IPCE) over 80%.^[9] In this paper we describe the syn-

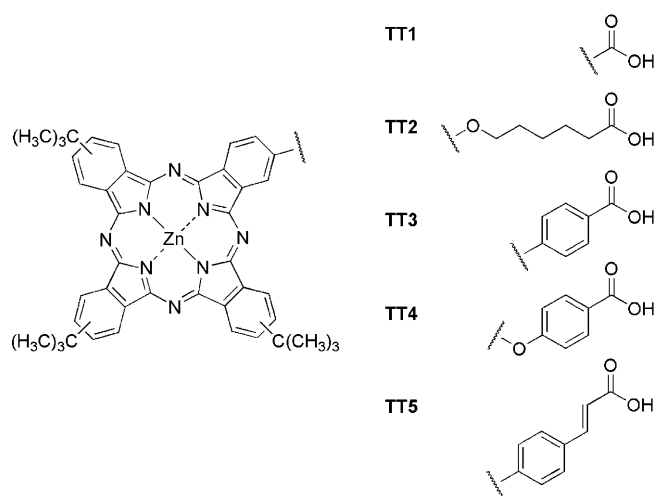
[a] Dr. J.-J. Cid, M. García-Iglesias, Prof. P. Vázquez, Prof. T. Torres
Departamento de Química Orgánica
Universidad Autónoma de Madrid, Cantoblanco
28049, Madrid (Spain)
Fax: (+34)914-973-966
E-mail: tomas.torres@uam.es

[b] Dr. J.-H. Yum, Prof. M. Grätzel, Prof. M. K. Nazeeruddin
Laboratory for Photonics and Interfaces
Institute of Chemical Sciences and Engineering
School of Basic Sciences
Swiss Federal Institute of Technology
1015 Lausanne (Switzerland)
Fax: (+41)216-934-111
E-mail: mdkhaja.nazeeruddin@epfl.ch

[c] A. Forneli, J. Albero, Dr. E. Martínez-Ferrero, Prof. E. Palomares
Institute of Chemical Research of Catalonia
ICIQ, Avda. Països Catalans 16, 43007 Tarragona (Spain)
Fax: (+34)977-920-223
E-mail: epalomares@icq.es

Supporting information for this article is available on the WWW under <http://dx.doi.org/10.1002/chem.200801778>.

thesis and characterisation of a series of unsymmetrical zinc phthalocyanines **TT1–TT5**, and the effect the spacer between the anchoring group and the TiO₂ surface has on photovoltaic properties.



Results and Discussion

Phthalocyanine synthesis: Phthalocyanines **TT1**,^[9] **TT2**,^[16] and **TT3**^[16] were prepared following a slightly modified procedure previously described by us. The phthalocyanines **TT4** and **TT5** were synthesised following the routes depicted in Schemes 1 and 2, respectively. Thus, unsymmetrical phthalocyanine **2** (Scheme 1) was prepared by a cyclotetramerisation reaction of 4-*tert*-butylphthalonitrile and substituted phthalonitrile **1**^[17] in a 4:1 ratio in the presence of zinc acetate (Zn(OAc)₂) and heated at reflux in dimethylaminoethanol (DMAE) to give 33% yield. The desired phthalocyanine was separated chromatographically as a mixture of

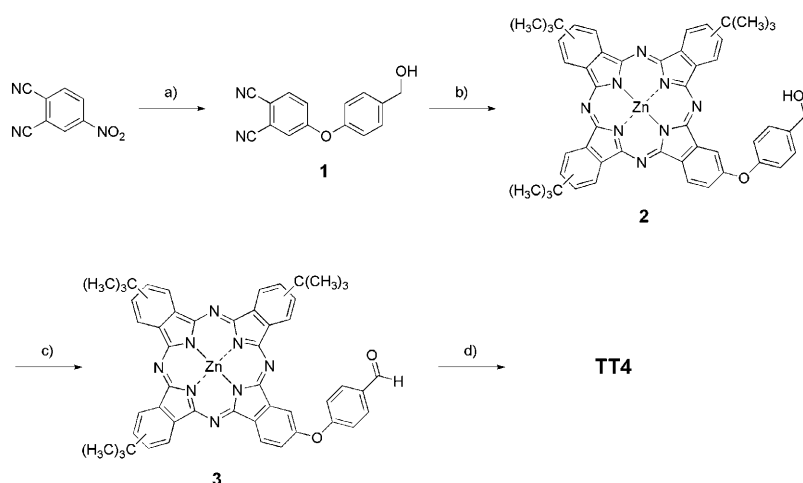
regioisomers from the reaction mixture. Further chemical modifications consisting of two oxidation steps were accomplished using the hydroxyl compound **2** to obtain carboxyphthalocyanine **TT4**. Two consecutive oxidations were necessary, since the direct oxidation from the alcohol to the carboxylic acids did not work under the common synthetic procedures. A very soft oxidation of the hydroxyl group in **2** with the periodinane derivative IBX (1-hydroxy-1,2-benziodoxole-3(1*H*)-one-1-oxide) in dimethyl sulfoxide (DMSO) afforded the formyl derivative **3** in 81% yield, after chromatographic isolation. Compound **3** was then treated with NaClO₂ in water, in the presence of sulfamic acid as a chlorine atom scavenger, leading to carboxyphthalocyanine **TT4** in 54% yield, after purification by chromatography on the reverse phase.

On the other hand, compound **TT5** was synthesised by means of palladium-catalysed cross-coupling reactions in a three-step synthetic sequence depicted in Scheme 2: Suzuki cross coupling reaction of iodophthalocyanine **4**^[18,19] with 4-bromophenylboronic acid and Pd(PPh₃)₄ (Ph = phenyl), afforded the bromo derivative **5** in moderate yield (34%). Compound **5** was then treated under Heck reaction conditions with [Pd(PPh₃)₄] in ethyl acrylate heated to reflux, giving rise to the ester derivative **6** in a 69% yield. Compound **6** was transformed in the last step to carboxyphthalocyanine **TT5** by hydrolysis with KOH, in high yield (90%) after chromatographic purification on the reverse phase.

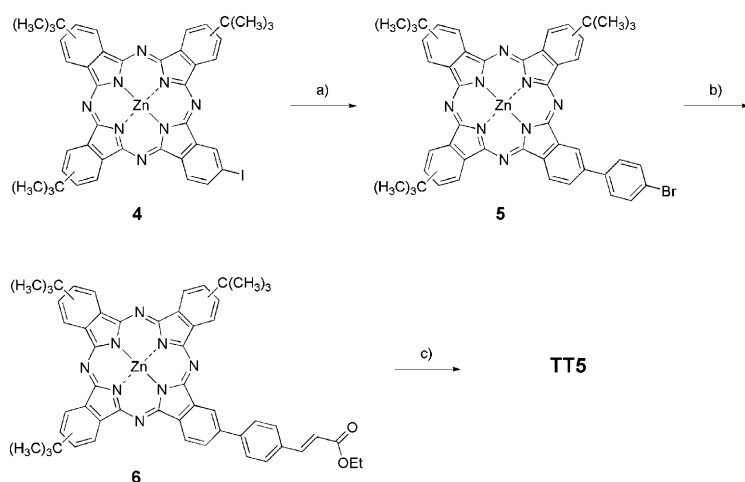
UV/Vis measurements: All the sensitizers are soluble in various polar solvents, such as dichloromethane, chloroform, tetrahydrofuran, methanol and ethanol. As an example, the normalised UV/Vis absorption spectrum for **TT3** sensitizer is shown in Figure 1. The different molecules have maximum absorbances in the near infrared region. Compounds **TT2** and **TT3** show a maximum absorbance in solution at 670 and 675 nm, respectively, while **TT4** and **TT5** show maximum absorbance peaks at 672 and 684 nm, respectively.

Moreover, the solid-state spectrum shows a broadening of the phthalocyanine Q-band, but no shift of their absorbance maximum. This enlargement is mainly due to the adsorption of the dye molecules onto the transparent mesoporous TiO₂ or Al₂O₃ films and suggests the lack of significant molecular aggregation, as will be illustrated by the IPCE measurements later in the paper.^[9]

Electrochemical, steady-state and lifetime emission measurements: When all phthalocyanines were excited within the Q-band (Q_b = 670–684 nm) in solution under ambient condi-



Scheme 1. Synthesis of phthalocyanine **TT4**. a) 4-(Hydroxymethyl)phenol, Cs₂CO₃, DMF; 65%. b) 4-*tert*-Butylphthalonitrile, Zn(OAc)₂, DMAE; 33%. c) IBX, DMSO; 81%. d) i) NaClO₂, acetone, ii) H₃NO₃S, H₂O; 54%.



Scheme 2. Synthesis of phthalocyanine **TT5**. a) 4-Bromophenylboronic acid, Pd(PPh₃)₄, K₂CO₃, DMF; 34%. b) Ethyl acrylate, [Pd(PPh₃)₄], K₂CO₃; 69%. c) KOH, dioxane; 90%.

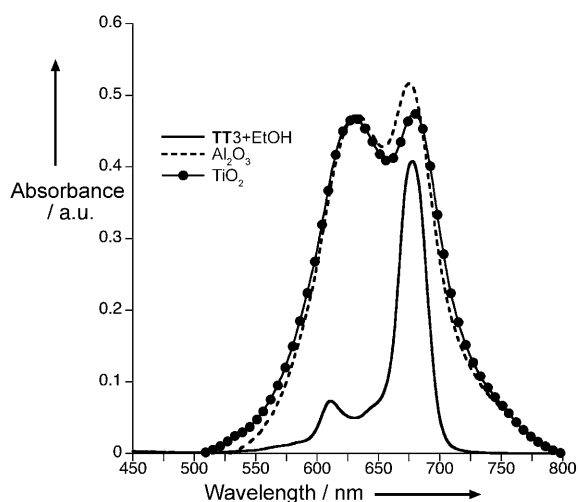


Figure 1. UV/Vis spectra of **TT3** phthalocyanine in ethanol (4×10^{-6} M) and adsorbed onto 4 μm thick films of Al₂O₃ and TiO₂.

tions, they exhibited a luminescence maximum between 680 and 695 nm. It is worth mentioning that the emission is strongly quenched when the dyes are adsorbed onto the TiO₂ film, which, in principle, is indicative of efficient electron injection. On the other hand, the cyclic voltammogram of the phthalocyanine dyes, for example, **TT3**, exhibited a quasi-reversible oxidation at $E_{1/2} = 0.74$ V versus SCE assigned to the phthalocyanine-ring oxidation processes. When scanning towards negative potentials, one reversible wave was observed at $E_{1/2} = -1.03$ V, which we assigned to the phthalocyanine-ring-based re-

duction, as it has been observed before.^[23] Table 1 contains all the relevant luminescence emission and electrochemical data for the phthalocyanine dyes in solution.

As previously reported by several groups, including ours,^[24–27] the use of time-correlated single-photon-counting (TCSPC) measurements is a convenient technique to estimate the yield of electron injection and also to approximately calculate the electron-injection kinetics when a sensitised wide-band-gap metal oxide is used as a reference for comparison purposes. The use of a large-band-gap metal

oxide such as ZrO₂ or Al₂O₃ prevents electron injection from an excited dye (lowest unoccupied molecular orbital: LUMO) into the metal oxide and, therefore, the energy of the excited state is radiatively dissipated before the dye relaxes to the ground state. Hence, if we use sensitised films with the same absorbance value at λ_{ex} (and hence similar dye coverage), and during the measurement of the emission lifetime we keep the acquisition time constant for the control and the sample, in our case the dye/Al₂O₃ and the dye/TiO₂, we can evaluate the yield of electron injection, as illustrated for **TT4** in Figure 2. The yields of electron injection for all of the dyes tested are higher than 90% with electron-injection kinetics in the range of 173–277 ps, calculated according to Koops et al.^[24] We note that the estimated lifetime corresponds to the fit of the experimental data, since the TCSPC instrument response is 325 ps measured at FWHM. In fact, this time range is in good agreement with the electron-injection studies carried out previously on Zn-based phthalocyanines, which showed injection dynamics of ≈ 250 ps. It is worth noting that for **TT1**, the phthalocyanine dye gives higher light-to-energy conversions that are faster with respect to other dyes (170 ps). Therefore, we conclude

Table 1. Luminescence emission and electrochemical properties of the tested phthalocyanines.

Sample	λ_{max} [nm]/ $\epsilon^{[a]}$ [mol ⁻¹ cm ⁻²]	λ_{em} [nm] ^[b]	τ (solution) [ns] ^[c]	τ (Al ₂ O ₃ films) [ns] ^[c]	$E_{1/2}$ vs. SCE [V] ^[d]
TT1 ^[e]	680	695	4 (40.5%) 2.8 (59.5%)	1.1 (81.4%) 2.8 (18.6%)	0.79
TT2	670/142 500	680	4.04 (100%)	2.8 (100%)	0.67
TT3	675/125 000	685	3.5 (100%)	3.3 (49.4%) 1.1 (50.6%)	0.74 -1.01
TT4	672/125 893	680	3.2 (89.1%) 3.8 (10.9%)	0.9 (100%)	0.8 -1.05
TT5	684/173 780	695	3.42 (100%)	1.5 (100%)	-

[a] λ_{max} = absorption maximum; ϵ : absorption extinction coefficient. [b] λ_{em} = Emission maximum; the samples were dissolved in THF. The excitation wavelength was $\lambda_{\text{ex}} = 650$ nm. [c] τ = Emission lifetime: Samples were excited at $\lambda_{\text{ex}} = 635$ nm and the emission was monitored at $\lambda_{\text{em}} = 700$ nm. [d] The samples were measured in THF with TBAP (0.1 M) as electrolyte and SCE as reference electrode. [e] From reference [9].

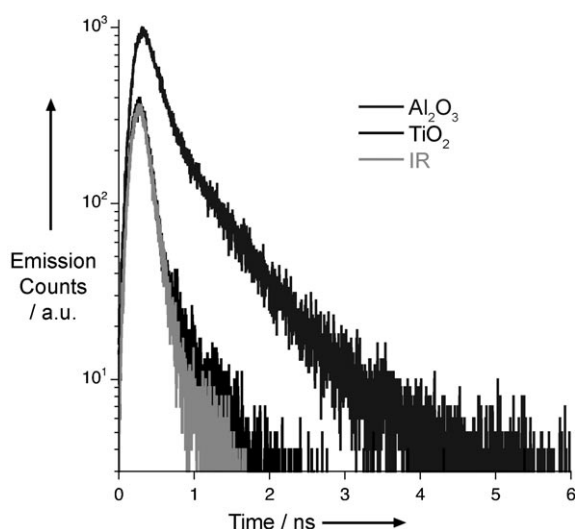


Figure 2. Time-correlated single photon counting measurements for **TT4**-sensitised Al_2O_3 and TiO_2 films ($\lambda_{\text{ex}}=635$ nm, $\lambda_{\text{em}}=700$ nm). IR stands for the instrument response (325 ps). The acquisition time was 1500 s. The sensitised film optical absorbance at $\lambda=635$ nm was 0.7 a.u. for both films.

that, in the case of phthalocyanine dyes, faster electron injection is a requisite and, thus, good orbital coupling and injection directionality between the dye and the titanium orbitals is a must.

Electron recombination kinetics: Once the electron-injection dynamics were determined, we turned to the recombination dynamics for the Zn-phthalocyanine, nanocrystalline- TiO_2 -sensitised films. We employed laser transient absorption spectroscopy (TAS) to measure the decay and the excited spectrum of the light-induced cation for the sensitised samples. To ensure similar dye coverage, all of the measured samples showed similar absorbance values at λ_{ex} . Figure 3 shows the typical data for the charge-recombination process measured by TAS, and can be fitted to a stretched exponential [$\Delta\text{O.D.}=\exp(-(t/\tau)^\alpha)$]. The stretched exponential kinetics has been discussed for a wide range of sensitizers employed in dye-sensitised solar cells (DSSC) and has been assigned to the presence of an inhomogeneous distribution of electron traps in the film.^[28–30] The recombination dynamics (lifetime, measured at half maximum of the signal, and α value) for the samples are shown in Table 2. In the cases of **TT1**, **TT2**, **TT4** and **TT5**, the electron recombination dynamics is ten times slower than that of the widely used ruthenium dye N719 (*cis*-bis(isothiocyanato)bis(2,2'-bipyridyl-4,4'-dicarboxylate)ruthenium(II) bis-tetrabutylammonium) that we found to give $t_{1/2}=0.28$ ms ($\alpha=0.34$). The fact that the recombination dynamics for the **TT** samples, except **TT3**, show a high value of α implies that the injected electrons had sufficient time to thermally equilibrate among all the available trap sites^[30,31] before they recombined with the oxidised dye, and, therefore, a quasi-monoexponential decay is observed. In the case of **TT3**, we did not observe a plateau at faster recombination timescales (μs), indicating

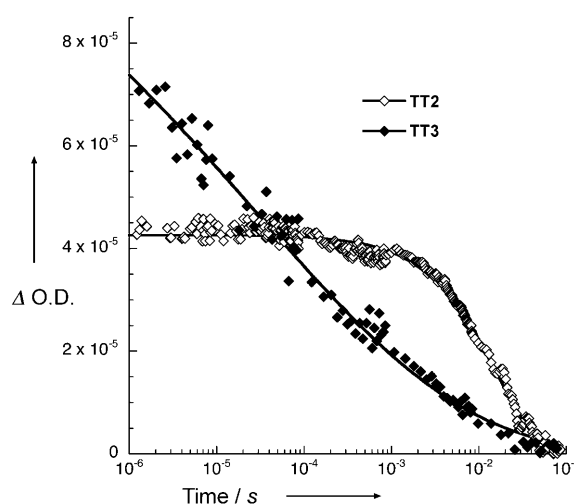


Figure 3. Electron recombination dynamics for a $4\ \mu\text{m}$ thick **TT2**- and **TT3**-sensitised mesoporous TiO_2 film. The sensitised film optical absorbance at the laser excitation wavelength ($\lambda_{\text{ex}}=520$ nm for **TT3**, $\lambda_{\text{ex}}=550$ nm for **TT2**) was 0.7 a.u. for each film. The probe wavelength for the measurement was fixed at $\lambda_{\text{probe}}=600$ nm. The fitting corresponds to a stretched exponential (see text for details).

Table 2. Electron recombination kinetic parameters and efficiency measurements of the tested phthalocyanines (see text for details).

Sample	$t_{1/2}$ [ms]	α ^[a]	J_{SC} [mA cm ⁻²] ^[b]	V_{OC} [mV] ^[b]	FF ^[b]	η [%] ^[b]
TT1	3.2	0.62	7.60 ± 0.20	617 ± 20	0.75 ± 0.02	3.52
TT2	11.7	0.9	0.90 ± 0.20	550 ± 10	0.72 ± 0.02	0.4
TT3	0.11	0.18	4.80 ± 0.20	610 ± 10	0.74 ± 0.02	2.20
TT4	5.2	0.97	1.44 ± 0.20	611 ± 10	0.75 ± 0.01	0.67
TT5	3.9	0.52	6.80 ± 0.20	613 ± 10	0.74 ± 0.01	3.10

[a] Calculated from the stretched exponential [$\Delta\text{O.D.}=\exp(-(t/\tau)^\alpha)$].
 [b] Short circuit photocurrent density (J_{SC}), open circuit voltage (V_{OC}), fill factor (FF), and overall conversion efficiency (η) related in the equation: $\eta=J_{\text{SC}}V_{\text{OC}}\text{FF}/P_{\text{in}}$ (P_{in} incident radiation power, mW cm^{-2}).

that the recombination process begins before we can measure. However, the fast electron injection dynamics for **TT3** avoids the potential kinetic competition between electron injection and electron recombination between the photo-injected electrons and the oxidised **TT3**.

The spectrum of the excited state for **TT2**/ TiO_2 and **TT3**/ TiO_2 was also recorded under ambient conditions. Both samples show similar features with a broad maximum at $\lambda=525$ nm, which we assign to the phthalocyanine cation after injection of one electron into the semiconducting band as other groups have previously reported.^[7,32]

On the other hand, we have carried out electron recombination kinetic studies in complete functional devices. Figure 4 shows the measured recombination lifetimes at different electron density for each device. It is worth noting that all devices were made by using the same TiO_2 thickness ($3\ \mu\text{m}$) as well as the same electrolyte (0.6 M 1-butyl-3-methylimidazolium iodide, 0.04 M iodine, 0.025 M LiI, 0.05 M guanidium thiocyanate, and 0.28 M *tert*-butylpyridine in a 15:85 (v/v) mixture of valeronitrile/acetonitrile). As can be seen,

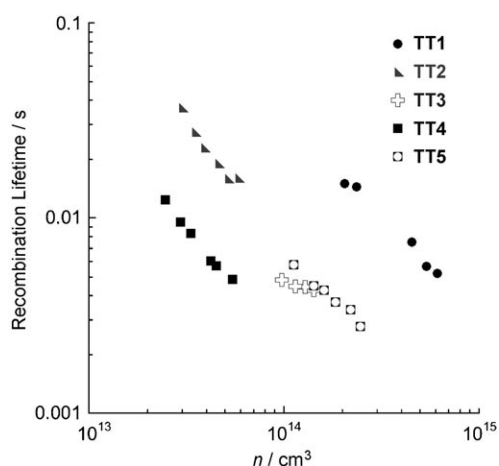


Figure 4. Electron recombination dynamics for a 4 μm thick **TT**-sensitized 1 cm^2 TiO_2 solar cell.

the differences between the devices are significant. For example, under the same experimental conditions, **TT2** and **TT4** show less charge (electrons) density than **TT1**, **TT3** and **TT5** devices. This fact makes the comparison between the different devices very difficult. However, we can already foresee that in the case of **TT2** and **TT4**, the latter shows faster recombination dynamics and, therefore, we should expect lower device performance not only in photocurrent but also in photovoltage. Moreover, according to the measured electron density, we can expect low photocurrent for the **TT2** devices when compared to **TT1**, **TT3** and **TT5**.

Dye-sensitised solar cells: The modification of the selected linker groups within the series **TT1–TT5** allows not only a variable distance between the dye and the photosensitised nanocrystalline TiO_2 , but also a distinct orientation of the dye molecular plane with regard to the semiconductor surface, which modifies the orbital coupling between the dyes and the semiconductor.^[33,34] To reduce aggregation of dye molecules, dye solution involving 60 (**TT1**) or 120 mM (**TT2–TT5**) 3*a*,7*a*-dihydroxy-5*b*-cholanic acid (CDCA) is used for sensitization process. Figure 5 shows the IPCE obtained with a sandwich cell by using *N*-methyl-*N*-butylimidazolium iodide (0.6M), iodine (0.04M), LiI (0.025M), guanidinium thiocyanate (0.05M) and *tert*-butylpyridine (0.28M) in 15:85 (v/v) mixture of valeronitrile and acetonitrile as redox electrolyte. The IPCE data of all sensitisers plotted as a function of excitation wavelength exhibit as low as 9% efficiency for **TT2** to extraordinarily high 85% efficiency for **TT1**.

Under standard global air mass (AM) 1.5 solar conditions, the **TT2**-sensitized cell gave a poor performance. We believe that this discouraging result is most probably due to the low directionality in the excited state of the sensitiser as well as the intrinsic properties of the linker, which has a non-conjugated and flexible moiety as an anchoring extension from the aromatic core of the phthalocyanine to the nanocrystalline surface of the semiconductor nanoparticle. In contrast, when the flexible and insulating bridge in **TT2** was replaced

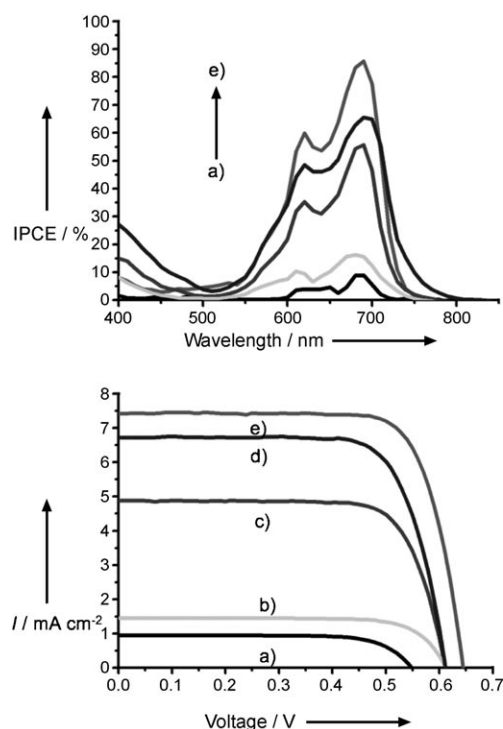


Figure 5. Photocurrent action spectrum (top) and current-voltage characteristics (bottom) of **TT1** (e), **TT2** (a), **TT3** (c), **TT4** (b), and **TT5** (d) obtained with a nanocrystalline TiO_2 film supported on a conducting glass sheet and derivatised with a monolayer of phthalocyanine sensitizers in the presence of chenodeoxycholic acid. A sandwich-type cell configuration was used to measure these spectra.

with a rigid and conducting bridge in **TT3**, the incident monochromatic photon-to-current conversion efficiency increased phenomenally from 9 to 56%. In fact, **TT3**, which has a rigid connection between the phthalocyanine moiety and the phenyl carboxylic unit, exhibits remarkable IPCE spectra due to the high directionality in the excited state of the sensitiser, which must be located perpendicular to the TiO_2 surface. On the other hand, **TT5** also has a rigid bridge with an extended conjugation and showed higher photovoltaic performance when compared to **TT3**. This result is caused by enhanced light-harvesting yield (molar extinction coefficient) of **TT5** due to the mentioned extended conjugation and slower recombination processes. These observations are in good agreement with the recombination kinetics carried out in the devices as explained above.

To prove the “directional effect,” **TT4**-sensitized solar cells were prepared. This low result is in total agreement with previous findings and is caused by poor electronic coupling of the phthalocyanine donor with TiO_2 d orbitals, because of the flexible and non-directional oxygen linker. Finally, when there is no bridge between the anchoring carboxylic acid group and the zinc phthalocyanine, like in **TT1**, the increase in the IPCE value is outstanding (85%) when compared to the **TT4** (IPCE 16%) and **TT5** (IPCE 65%) sensitizers. The **TT1** sensitiser under standard global AM 1.5 solar conditions yielded a total efficiency of 3.55%. The im-

proved efficiency of the **TT1** compared to the **TT5**, **TT3**, **TT4** and **TT2** sensitizers (in this order) demonstrates the influence the nature of the bridge between the anchoring carboxylic acid group and zinc phthalocyanine.

To the best of our knowledge, these data provide a major breakthrough in the design and development of near-infrared-based sensitizers. Therefore, we believe that the findings of this study should spark a broad spectrum of interest in molecular engineering of low-band-gap sensitizers for solar cells.

Conclusion

In summary, we have developed a series of phthalocyanine sensitizers, which demonstrate the impact of anchoring group on photovoltaic performance, yielding power conversion efficiencies from 0.4 to 3.55% under light-simulated 1.5 AM irradiation conditions. Also, our finding demonstrates that creating directionality in the excited state of the sensitizer by adjusting the electron densities of donor moieties and the anchoring group is the key for the unprecedented efficiency of **TT1** and probably for the design of future red-light-absorbing molecular materials. Moreover, we found that faster electron injection kinetics are needed with these dyes in order to achieve higher efficiencies. These faster electron-injection kinetics are directly related to the directionality (orbital coupling) of these dyes. Further work is being carried out to increase the overlap between the dyes' LUMO and the 3d titanium orbitals through modification of the peripheral anchoring ligands.

Experimental Section

Phthalocyanines **TT1**,^[9] **TT2**,^[16] and **TT3**^[16] were prepared following slightly modified procedures previously described by us.

4-[4-(Hydroxymethyl)phenoxy]phthalonitrile (1): 4-Nitrophthalonitrile (1.00 g, 5.77 mmol) and Cs₂CO₃ (3.76 g, 11.54 mmol) in anhydrous DMF (50.0 mL) were stirred under argon for 15 min. Then, 4-(hydroxymethyl)phenol (1.43 g, 11.54 mmol) was added slowly in a few portions, and the mixture was heated at 40 °C for 72 h. After cooling, the yellow-greenish suspension was added to brine (300 mL) and extracted with diethyl ether (5 × 50 mL). The organic extracts were washed with brine (50 mL) and dried over Na₂SO₄. The drying agent was removed by filtration and the solvent evaporated in vacuum. The resulting yellow-green oily crude was purified by column chromatography over silica gel by using ethyl acetate (EtOAc) as an eluent. Compound **1** was obtained as a yellow oil (0.94 g, 65%) that solidifies upon standing. M.p. 75–77 °C; ¹H NMR (300 MHz, CDCl₃, 25 °C, TMS): δ = 2.25 (brs, 1H; CH₂OH), 4.74 (s, 2H; CH₂OH), 7.07 (d, ³J = 8.6 Hz, 2H; H-3', H-5'), 7.24 (dd, ³J = 8.3 Hz, ⁴J = 2.6 Hz, 1H; H-5), 7.26 (d, ⁴J = 2.6 Hz, 1H; H-3), 7.47 (d, ³J = 8.6 Hz, 2H; H-2', H-6'), 7.72 ppm (d, ³J = 8.3 Hz, 1H; H-6); ¹³C NMR (75 MHz, CDCl₃): δ = 68.1 (CH₂OH), 108.9 (C-1), 115.1 (C-2), 115.5 (2 × CN), 117.7 (C-2', C-6'), 120.8 (C-3), 121.6 (C-5), 129.3 (C-3', C-5'), 135.6 (C-6), 139.3 (C-4'), 152.9 (C-1'), 162.0 ppm (C-4); FTIR (KBr): $\tilde{\nu}$ = 3472 (O-H, associated dimer), 3072, 3045 (O-H, non-associated dimer), 2945, 2878, 2235 (C≡N), 1603, 1495, 1427, 1263, 1247, 1207, 1099, 1045, 1018, 951, 897, 843 cm⁻¹; MS (EI): *m/z* (%): 251 (97) [*M*]⁺, 249 (38) [*M*-H]⁺, 234 (19) [*M*-OH]⁺, 221 (96) [*M*+H-CH₂OH]⁺, 192 (40) [*M*₂+H-HCN]⁺, 107 (100) [C₇H₇O]⁺.

9(10),16(17),23(24)-Tri-tert-butyl-2-[4-(hydroxymethyl)phenoxy]phthalocyaninatozinc(II) (mixture of regioisomers) (2): Phthalonitrile **1** (1.23 mmol), 4-tert-butylphthalonitrile (907 mg, 4.92 mmol) and Zn(OAc)₂ (300 mg, 1.64 mmol) were stirred in DMAE (7.0 mL) and heated at reflux under an argon atmosphere for 18 h. After cooling to room temperature, the intense blue solution was poured into water (150 mL) and the precipitate collected by filtration through celite. The resulting blue solid was washed with water, methanol/water mixtures (1:2) and (1:1) (100 mL each) and finally with MeOH (50 mL). Afterwards, the dried solid was redissolved in THF and purified by column chromatography on silica gel using hexane/dioxane (2:1) and (1:1) as eluent. The isolated blue solid was triturated in hot hexane, filtered and dried to afford **2** as a dark blue solid (352 mg, 33%). M.p. >250 °C; ¹H NMR (500 MHz, [D₆]DMSO, 25 °C, TMS): δ = 1.9–1.7 (s, 27H; C(CH₃)₃), 4.66 (m, 2H; CH₂OH), 5.32 (m, 1H; CH₂OH), 7.8–7.5 (m, 4H; ArH), 8.4–8.1 (m, 4H; PcH), 9.3–8.6 ppm (m, 8H; PcH); UV/Vis (THF): λ_{max}(log ε) = 350 (4.9), 608 (4.5), 673 nm (5.3); MS (MALDI-TOF, dithranol): *m/z* (%): 873–866 (100) [*M*]⁺; HR MALDI-TOF MS, dithranol: *m/z* calcd for C₅₁H₄₆N₈O₂Zn: 866.30352; found: 866.30297 [*M*]⁺; elemental analysis calcd (%) for C₅₁H₄₆N₈O₂Zn (866.30352): C 70.54, H 5.34, N 12.90; found: C 70.60, H 5.35, N 12.89.

9(10),16(17),23(24)-Tri-tert-butyl-2-[4-formyl]phenoxy]phthalocyaninatozinc(II) (mixture of regioisomers) (3): Compound **2** (0.195 mmol) was added to a well stirred and colourless solution of periodinane 1-hydroxy-1,2-benziodoxole-3(1*H*)-one-1-oxide (IBX) (112 mg, 0.312 mmol) in DMSO (47.0 mL) at room temperature. The solution was stirred at room temperature for 5 h and then, poured over brine (200 mL) and extracted with Et₂O (3 × 40 mL). The organic layer was separated, washed with a saturated aqueous solution of NaHCO₃ (2 × 60 mL) and brine (2 × 60 mL), and dried over Na₂SO₄. After filtration of the drying agent, the solvent was evaporated and the blue solid was purified by column chromatography on silica gel using hexane/dioxane (3:1) as eluent, affording aldehyde **3** as a dark blue solid (137 mg, 81%). M.p. >250 °C; ¹H NMR (500 MHz, [D₆]DMSO, 25 °C, TMS): δ = 1.8–1.7 (m, 27H; C(CH₃)₃), 7.8–7.6 (m, 4H; ArH), 9.3–8.1 (m, 12H; PcH), 10.1–9.9 ppm (m, 1H; CHO); FTIR (KBr): $\tilde{\nu}$ = 2961, 2907, 2866, 1705 (C=O), 1597, 1485, 1404, 1337, 1242, 1163, 1095, 1055, 947, 831, 758, 696, 530 cm⁻¹; UV/Vis (THF): λ_{max}(log ε) = 349 (4.9), 607 (4.6), 672 nm (5.4); MS (MALDI-TOF, dithranol): *m/z* (%): 871–864 (100) [*M*]⁺; HR MALDI-TOF MS, dithranol: *m/z* calcd for C₅₁H₄₄N₈O₂Zn: 864.28787; found: 864.28732 [*M*]⁺; elemental analysis calcd (%) for C₅₁H₄₄N₈O₂Zn (864.28787): C 70.71, H 5.12, N 12.93; found: C 70.73, H 5.10, N 12.98.

9(10),16(17),23(24)-Tri-tert-butyl-2-[4-carboxy]phenoxy]phthalocyaninatozinc(II) (mixture of regioisomers) (TT4): NaClO₂ (47 mg, 0.50 mmol) was added in a few portions to a vigorously stirred solution of aldehyde **3** (0.17 mmol) cooled to 0 °C in acetone (96 mL). Then, a solution of sulfamic acid (51 mg, 0.50 mmol) in Milli-Q grade deionised water (12 mL) was added all in one portion. The reaction was allowed to proceed at room temperature for 4 h. After the starting compound had disappeared, the solution was poured into aqueous HCl (0.1 M, 400 mL) and a blue-green solid precipitated. The solid was filtered over celite and washed with water and mixtures of water/MeOH (3:1 and 2:1, 100 mL each). Then, it was dried under vacuum and extracted with THF. The solvent was evaporated, and the crude product was triturated in hexane, filtered, and washed with a solution of water/MeOH (1:1, 50 mL) and finally with cold MeOH (25 mL) to afford a dark blue solid. Further purification was accomplished by column chromatography (reverse phase) employing water/THF (1:1) as eluent affording **TT4** (81 mg, 54%). M.p. >250 °C; ¹H NMR (500 MHz, [D₆]DMSO, 25 °C, TMS): δ = 1.9–1.5 (s, 27H; C(CH₃)₃), 9.7–7.0 (m, 16H; PcH, ArH), 12.85 ppm (brs, 1H; CHO); FTIR (KBr): $\tilde{\nu}$ = 3418, 2959, 2878, 1711, 1603, 1475, 1394, 1327, 1320, 1165, 1084, 930, 837, 748, 698, 528, 446 cm⁻¹; UV/Vis (THF): λ_{max}(log ε) = 349 (4.9), 607 (4.6), 672 nm (5.3); MS (MALDI-TOF, dithranol): *m/z* (%): 887–880 (100) [*M*]⁺; HR MALDI-TOF MS, dithranol: *m/z* calcd for C₅₁H₄₄N₈O₃Zn: 880.28278; found: 880.28224 [*M*]⁺; elemental analysis calcd (%) for C₅₁H₄₄N₈O₃Zn (880.28278): C 69.42, H 5.03, N 12.70; found: C 69.45, H 5.00, N 12.78.

9(10),16(17),23(24)-Tri-tert-butyl-2-[(4-bromo)phenyl]phthalocyaninatozinc(II) (mixture of regioisomers) (5): A mixture of iodophthalocyanine **4** (40.0 mg, 0.046 mmol), 4-bromophenylboronic acid (10.2 mg, 0.051 mmol), [Pd(PPh₃)₄] (26.6 mg, 0.023 mmol) and K₂CO₃ (17.7 mg, 0.128) in anhydrous DMF (4.0 mL) was heated at 45 °C under argon for 18 h. The solution was then poured into brine (150 mL) and extracted with Et₂O (2 × 50 mL). The organic extracts were washed with brine (2 × 30 mL), dried over MgSO₄ and filtered. After evaporation of the solvent, compound **5** was separated from the remaining iodophthalocyanine by using a chromatographic column (SiO₂, hexane/dioxane (3:1); the eluent polarity was gradually increased to 2:1). The obtained solid was triturated in methanol and hexane, filtered and dried, yielding **5** as a dark blue solid (14.0 mg, 34%). M.p. >250 °C; ¹H NMR (500 MHz, [D₆]DMSO, 25 °C, TMS): δ = 1.9–1.7 (s, 27H, C(CH₃)₃), 8.5–7.1 (m, 13H, PcH), 9.5–8.9 ppm (m, 3H; PcH); UV/Vis (THF): λ_{max}(log ε) = 349 (4.6), 611 (4.3), 676 nm (5.0); MS (MALDI-TOF, dithranol): *m/z* (%): 908–899 (100) [*M*]⁺; elemental analysis calcd (%) for C₅₀H₄₄BrN₈Zn: C 66.56, H 4.92, N 12.42; found: C 66.66, H 4.92, N 12.39.

(E)-9(10),16(17),23(24)-Tri-tert-butyl-2-[4-[2-(ethyl)acryloyl]phenyl]phthalocyaninatozinc(II) (mixture of regioisomers) (6): Bromophenylphthalocyanine **5** (20.0 mg, 0.022 mmol), [Pd(PPh₃)₄] (12.7 mg, 0.011 mmol) and K₂CO₃ (8.3 mg, 0.060 mmol) were heated to reflux in ethyl acrylate (3.0 mL) for 18 h in an argon atmosphere. After cooling to room temperature, excess ethyl acrylate was removed under vacuum and the crude was purified by column chromatography on silica gel using hexane/dioxane (2:1) as eluent to yield **6** (14.0 mg, 69%) as a dark blue solid. M.p. >250 °C; ¹H NMR (500 MHz, [D₆]DMSO, 25 °C, TMS): δ = 1.7–1.6 (s, 27H; (CH₃)₃), 6.51 (d, ³*J* = 16.8 Hz, 1H; ArCH=CHCO₂Et), 7.62 (d, ³*J* = 16.8 Hz, 1H; ArCH=CHCO₂Et), 7.79 (br s, 2H; ArH), 8.4–8.0 (m, 6H; PcH, ArH), 9.5–9.0 ppm (m, 8H; PcH); FTIR (KBr): ν̄ = 2959, 2876, 1715, 1634, 1487, 1460, 1393, 1366, 1313, 1261, 1167, 1126, 1099, 980, 806, 459 cm⁻¹; UV/Vis (THF): λ_{max}(log ε) = 352 (4.9), 610 (4.5), 672, (5.2), 685 nm (5.2); MS (MALDI-TOF, dithranol): *m/z* (%): 925–918 (100) [*M*]⁺; elemental analysis calcd. (%) for C₅₅H₅₀N₈O₂Zn: C 71.77, H 5.48, N 12.17; found: C 71.73, H 5.55, N 12.21.

(E)-9(10),16(17),23(24)-Tri-tert-butyl-2-[(4-acryloyl)phenyl]phthalocyaninatozinc(II) (mixture of regioisomers) (TT5): An aqueous solution (3.0 mL) of KOH (8.4 mg, 0.150 mmol) was added dropwise to a stirred solution of ester **6** (14.0 mg, 0.015 mmol) in dioxane (25 mL). The mixture was then heated at reflux in an argon atmosphere for 1 h. After cooling, a solution of HCl (0.1 M) was added dropwise until pH < 5. The dark green mixture was poured into brine (125 mL), extracted with Et₂O (3 × 20 mL) and dried over Na₂SO₄. After filtration of the drying agent, the solvents were removed under and the crude product was purified on a chromatographic column (reverse phase, THF/water 5:2). In this way carboxyphthalocyanine **TT5** was afforded as a dark blue-green solid (12.0 mg, 90%). M.p. >250 °C; ¹H NMR (500 MHz, [D₆]DMSO, 25 °C, TMS): δ = 1.7–1.6 (s, 27H; C(CH₃)₃), 6.49 (d, ³*J* = 16.8 Hz, 1H; ArCH=CHCO₂H), 7.55 (d, ³*J* = 16.8 Hz, 1H; ArCH=CHCO₂H), 7.79 (m, 2H; ArH), 8.3–8.0 (m, 6H; PcH, ArH), 9.5–9.0 (m, 8H; PcH), 11.97 ppm (brs, 1H; COOH); FTIR (KBr) ν̄ = 3412, 2957, 2930, 2862, 1697, 1634, 1447, 1433, 1393, 1367, 1329, 1288, 1261, 1198, 1157, 1090, 1049, 930, 825, 756, 698 cm⁻¹; UV/Vis (THF): λ_{max}(log ε) = 352 (4.9), 611 (4.5), 673 (5.2), 684 nm (5.2); MS (MALDI-TOF, dithranol): *m/z* (%): 897–890 (100) [*M*]⁺; HR MALDI-TOF MS, dithranol: *m/z* calcd for C₅₃H₄₆N₈O₂Zn: 890.30352; found: 890.30297 [*M*]⁺; elemental analysis calcd (%) for C₅₃H₄₆N₈O₂Zn (890.30352): C 71.33, H 5.20, N 12.56; found: C 71.39, H 5.23, N 12.61.

UV/Vis and emission fluorescence measurements: The UV/Vis spectra of all the phthalocyanine dyes in THF (HPLC degree) were recorded on a Shimadzu UV/Vis system model 1700. The fluorescence emission properties of the dyes, either in solution or adsorbed onto the metal oxide films, were measured under ambient conditions using an Aminco Bowman Series 2 luminescence spectrometer equipped with a temperature controller and a holder for films and solid samples.

Nanocrystalline TiO₂ and Al₂O₃ films for optical measurements: The metal oxide nanoparticles were sensitised as reported previously.^[20] In brief, Al₂O₃ nanoparticles were purchased from Alfa-Aesar chemical

(20% in H₂O, colloidal dispersion). The colloidal dispersion (15 mL) was mixed with hydroxypropyl cellulose (0.35 g; 2 wt % of Al₂O₃). The mixture was stirred for 7 d at 65 °C. For the TiO₂ colloids, we followed previous literature reports.^[20] To prepare the transparent mesoporous metal oxide films, transparent glass cover slides were cleaned and a drop of the corresponding metal oxide paste was spread using a glass rod. After drying the films in air, the films were calcined at 450 °C for 30 min. The measured thickness was 4 μm.

Electron recombination measurements: Laser transient absorption spectroscopy was used to determine the recombination lifetimes of **TT1–TT5** phthalocyanine-sensitised TiO₂ films. All the films had the same absorbance value. The experiments were carried out as reported before.^[15] Briefly, a PTI nitrogen dye laser model was used as excitation source with the appropriated dye solution. The laser power was kept constant during the experiment to 0.05 mJ cm⁻² with a repetition rate of 1 Hz (pulse duration less than 1 ns). The resulting photoinduced change in optical density was monitored by using a 150 W tungsten lamp with 20 nm bandwidth PTI monochromators before and after the sample, a photodiode-based detection system from Costronic Electronics and a TDS-220 Tektronic DSO oscilloscope.

Electron injection measurements: Time-correlated single-photon-counting measurements of complete DSSC devices were carried out by using an Edinburgh Instruments system model LifeSpec-PS. As an excitation source we used a picosecond laser diode λ_{ex} = 635 nm (laser power 2 nJ cm⁻² by pulse) with an instrument response of 325 ps FWHM (full width at half maximum). The devices were made using a 4 μm thick transparent film sensitised with the corresponding phthalocyanine dyes. The electrolyte was composed of a solution of 1-propyl-2,3-dimethylimidazolium iodide (DMPII; 0.60 M), iodide (0.04 M), lithium iodide (0.025 M), in a mixture of acetonitrile and valeronitrile (85:15 volume ratio). As control samples, we utilised Al₂O₃-sensitised films with identical absorbance at the excitation wavelength. The high conduction band of Al₂O₃ prevents the electron injection from the dye-excited state. The calculation of the injection yield was done by comparison of the area under the signal area of the control and the sample.

Electrochemical measurements: Measurements were done by cyclic voltammetry in a conventional three-electrode cell connected to a CH Instruments 660c potentiostat-galvanostat. We used tetrabutyl ammonium perchlorate (TBAP) as the electrolyte, a platinum working electrode, a calomel reference electrode (SCE) and a platinum wire as an auxiliary electrode. The 0.5 × 10⁻⁴ M solutions of the samples in THF were purged with Ar for 5 min prior to the measurements.

Dye-sensitised solar cells: The screen-printed double-layer film of TiO₂ consisted of a 9–10 μm transparent layer and a 4 μm scattering layer and were prepared and treated with titanium tetrachloride solution (0.05 M) using a previously reported procedure.^[21,22] The film was heated to 500 °C in air and calcined for 20 min before use. Dye solutions were prepared in the concentration range of 0.5–1 × 10⁻⁴ M solution in ethanol containing 3α,7α-dihydroxy-5β-cholanic acid (Cheno; 60 (**TT1**) or 120 mM (**TT2–TT5**)). The electrodes were soaked in the dye solution for 4 h at 22 °C and the dye-coated electrodes were rinsed quickly with ethanol and used as such for photovoltaic measurements. The electrolyte was composed of *N*-methyl-*N*-butyl imidazolium iodide (0.6 M), iodine (0.04 M), LiI (0.025 M), guanidinium thiocyanate (0.05 M) and *tert*-butylpyridine (0.28 M) in 15:85 (v/v) mixture of valeronitrile and acetonitrile. The dye-adsorbed TiO₂ electrode and the thermally platinised counter electrode were assembled into a sealed sandwich type cell with a gap of a hot-melt ionomer film (Surlyn 1702, 25 μm thickness, Du-Pont). To reduce scattered light from the edge of the glass electrodes of the dyed TiO₂ layer, a light-shading mask was used on the DSSCs, so the active area was fixed to 0.2 cm². For photovoltaic measurements of the DSSCs, the irradiation source was a 450 W xenon light source (Osram XBO 450, USA) with a Tempax 113 solar filter (Schott). The output power of an AM 1.5 solar simulator was calibrated by using a reference Si photodiode equipped with a coloured matched IR cut-off filter (KG-3, Schott) in order to reduce the mismatch in the region of 350–750 nm between the simulated light and AM 1.5 to less than 2%. The measurement delay time of photo I-V characteristics of DSSCs was fixed to 40 ms. The measurement of in-

cident photon-to-current conversion efficiency (IPCE) was plotted as a function of excitation wavelength by using the incident light from a 300 W xenon lamp (ILC Technology, USA), which was focused through a Gemini-180 double monochromator (Jobin Yvon Ltd.).

Acknowledgements

This work has been supported by the Spanish MEC (CTQ-2008-00418-BQU, CTQ2007-60746/BQU, CONSOLIDER-INGENIO 2010, NANOCIENCIA MOLECULAR-CSD2007-00010 and HOPE-CSD-0007-2007), the Comunidad de Madrid (S-0505/PPQ/000225), the EU (ROBUST DSC, Collaborative Research Project, 1 FP7-ENERGY-2007-1-RTD) and the ESF-MEC (MAT2006-2818-E, SOHYDS). E.M.F. acknowledges the MEC for her Juan de la Cierva Fellowship, and J.-H.Y. thanks the Korea Foundation for International Cooperation of Science & Technology through the Global Research Lab (GRL) program funded by the Ministry of Science and Technology.

- [1] G. de la Torre, C. G. Claessens, T. Torres, *Chem. Commun.* **2007**, 2000; Y. Rio, M. S. Rodríguez-Morgade, T. Torres, *Org. Biomol. Chem.* **2008**, *6*, 1877.
- [2] M. K. Nazeeruddin, R. Humphry-Baker, M. Grätzel, B. A. Murrer, *Chem. Commun.* **1998**, 719.
- [3] M. K. Nazeeruddin, R. Humphry-Baker, M. Grätzel, D. Wöhrle, G. Schnurpfeil, G. Schneider, A. Hirth, N. Trombach, *J. Porphyrins Phthalocyanines* **1999**, *3*, 230.
- [4] Y. Amao, T. Komori, *Langmuir* **2003**, *19*, 8872.
- [5] P. Panayotatos, D. Parikh, R. Sauer, G. Bird, A. Piechowski, S. Husain, *Sol. Cells* **1986**, *18*, 71.
- [6] J. Fang, J. Wu, X. Lu, Y. Shen, Z. Lu, *Chem. Phys. Lett.* **1997**, *270*, 145.
- [7] J. He, G. Benkoe, F. Korodi, T. Polivka, R. Lomoth, B. Kermack, L. Sun, A. Hagfeldt, V. Sundstrom, *J. Am. Chem. Soc.* **2002**, *124*, 4922.
- [8] K. Kato, M. Hirano, F. Takahashi, K. Shinbo, F. Kaneko, T. Wakamatsu, *Trans. Mater. Res. Soc. Jpn.* **2004**, *29*, 775.
- [9] J.-J. Cid, J.-H. Yum, S.-R. Jang, M. K. Nazeeruddin, E. Martínez-Ferrero, E. Palomares, J. Ko, M. Graetzel, T. Torres, *Angew. Chem.* **2007**, *119*, 8510; *Angew. Chem. Int. Ed.* **2007**, *46*, 8358; J.-H. Yum, S.-R. Jang, R. Humphry-Baker, M. Graetzel, J.-J. Cid, T. Torres, M. K. Nazeeruddin, *Langmuir* **2008**, *24*, 5636.
- [10] P. Y. Reddy, L. Giribabu, C. Lyness, H. J. Snaith, C. Vijaykumar, M. Chandrasekharam, M. Lakshmikantam, J.-H. Yum, K. Kalyanasundaram, M. Graetzel, M. K. Nazeeruddin, *Angew. Chem.* **2007**, *119*, 377; *Angew. Chem. Int. Ed.* **2007**, *46*, 373.
- [11] G. Liu, A. Klein, A. Thissen, W. Jaegermann, *Surf. Sci.* **2003**, *539*, 37.
- [12] V. Aranyos, J. Hjelm, A. Hagfeldt, H. Grennberg, *J. Porphyrins Phthalocyanines* **2001**, *5*, 609.
- [13] J. He, A. Hagfeldt, S.-E. Linquist, *Langmuir* **2001**, *17*, 2743.
- [14] A. Morandeira, I. López-Duarte, M. V. Martínez-Díaz, B. O'Regan, C. Shuttle, N. A. Haji-Zainulabidin, T. Torres, E. Palomares, J. R. Durrant, *J. Am. Chem. Soc.* **2007**, *129*, 9250.
- [15] E. Palomares, M. V. Martínez-Díaz, S. A. Haque, T. Torres, J. R. Durrant, *Chem. Commun.* **2004**, 2112.
- [16] J.-J. Cid, Ph.D. Thesis, Universidad Autónoma de Madrid, Madrid, **2008**.
- [17] B. Ballesteros, S. Campidelli, G. de la Torre, C. Ehli, D. M. Guldi, M. Prato, T. Torres, *Chem. Commun.* **2007**, 2950.
- [18] E. M. Maya, P. Vázquez, T. Torres, *Chem. Eur. J.* **1999**, *5*, 2004.
- [19] E. M. Maya, P. Haisch, P. Vázquez, T. Torres, *Tetrahedron* **1998**, *54*, 4397.
- [20] S. Hore, E. Palomares, H. Smit, N. J. Bakker, P. Comte, P. Liska, K. R. Thampi, J. M. Kroon, A. Hinsch, J. R. Durrant, *J. Mater. Chem.* **2005**, *15*, 412.
- [21] M. K. Nazeeruddin, P. Péchy, T. Renouard, S. M. Zakeeruddin, R. Humphry-Baker, P. Comte, P. Liska, C. Le, V. Shklover, L. Spiccia, G. B. Deacon, C. A. Bignozzi, M. Grätzel, *J. Am. Chem. Soc.* **2001**, *123*, 1613.
- [22] M. K. Nazeeruddin, F. de Angelis, S. Fantacci, A. Selloni, G. Viscardi, P. Liska, S. Ito, T. Bessho, M. Grätzel, *J. Am. Chem. Soc.* **2005**, *127*, 16835.
- [23] P. Matlaba, T. Nyokong, *Polyhedron* **2002**, *21*, 2463.
- [24] S. E. Koops, J. R. Durrant, *Inorg. Chim. Acta* **2008**, *361*, 663.
- [25] V. Biju, M. Micic, D. Hu, H. P. Lu, *J. Am. Chem. Soc.* **2004**, *126*, 9374.
- [26] S. Tatay, S. A. Haque, B. C. O'Regan, J. R. Durrant, W. J. H. Verhees, J. M. Kroon, A. Vidal-Ferran, P. Gavina, E. Palomares, *J. Mater. Chem.* **2007**, *17*, 3037.
- [27] C.-W. Chang, C. K. Chou, I.-J. Chang, Y.-P. Lee, E. W.-G. Diau, *J. Phys. Chem. C* **2007**, *111*, 13288.
- [28] J. R. Durrant, S. A. Haque, E. Palomares, *Chem. Commun.* **2006**, 3279.
- [29] J. R. Durrant, S. A. Haque, E. Palomares, *Coord. Chem. Rev.* **2004**, *248*, 1247.
- [30] H. N. Gohsh, J. B. Absury, Y.-X. Weng, T. Lian, *J. Phys. Chem. B* **1998**, *102*, 10208.
- [31] Y.-X. Weng, Y.-Q. Wang, J. B. Absury, H. N. Gohsh, T. Lian, *J. Phys. Chem. B* **2000**, *104*, 93.
- [32] P. Charlesworth, T. G. Truscott, R. C. Brooks, B. C. Wilson, *J. Photochem. Photobiol. B* **1994**, *26*, 277.
- [33] P. Piotrowiak, E. Galoppini, D. Wang, M. Myahkostupov, *J. Chem. Phys.* **2007**, *126-127*, 2827.
- [34] J. Rochford, D. Chu, A. Hagfeldt, E. Galoppini, *J. Am. Chem. Soc.* **2007**, *129*, 4655.

Received: August 28, 2008

Revised: December 31, 2008

Published online: March 31, 2009